NASA TECHNICAL MEMORANDUM

NASA TM X-3446

NASA TM X-3446

INTERNAL FLOW CHARACTERISTICS OF A MULTISTAGE COMPRESSOR WITH INLET PRESSURE DISTORTION

Claude E. deBogdan, John E. Moss, Jr., and Willis M. Braithwaite

Lewis Research Center
Cleveland, Ohio 44135

NATIONAL AERONAUTICS AND SPACE ADMINISTRATION • WASHINGTON, D. C. • FEBRUARY 1977

1. Report No. NASA TM X-3446	2. Government Accession No.	3. Recipient's Catalog No.
4. Title and Subtitle INTERNAL FLOW CHARACTERISTICS OF A MULTISTAGE COMPRESSOR WITH INLET PRESSURE DISTORTION		5. Report Date February 1977 6. Performing Organization Code
7. Author(s) Claude E. deBogdan, John E. Moss, Jr., and Willis M. Braithwaite		8. Performing Organization Report No. E-8848 10. Work Unit No. 505-05
9. Performing Organization Name and Address Lewis Research Center, National Aeronautics and Space Administration, Cleveland, Ohio 44135		11. Contract or Grant No. 13. Type of Report and Period Covered Technical Memorandum
12. Sponsoring Agency Name and Address National Aeronautics and Space Administration, Washington, D.C. 20546		14. Sponsoring Agency Code
15. Supplementary Notes		

16. Abstract

The measured distribution of compressor interstage pressures and temperatures resulting from a 180° inlet-total-pressure distortion for a J85-13 turbojet engine are reported. Extensive inner stage instrumentation combined with stepwise rotation of the inlet distortion gave data of high circumferential resolution. The steady-state pressures and temperatures along with the amplitude, extent, and location of the distorted areas are given. Data for 80, 90, and 100 percent of rotor design speed are compared with clean (undistorted) inlet flow conditions to show pressure and temperature behavior within the compressor. Both overall and stagewise compressor performances vary only slightly when clean and distorted inlet conditions are compared. Total- and static-pressure distortions increase in amplitude in the first few stages of the compressor and then attenuate fairly uniformly to zero at the discharge. Total-temperature distortion induced by the pressure distortion reached a maximum amplitude by the first two stages and decayed only a little through the rest of the compressor. Distortion amplitude tended to peak in line with the screen edges and, except for total and static pressure in the tip zone, there was little swirl in the axial direction.

17. Key Words (Suggested by Author(s))	18. Distribution Statement
Turbojet Compressor Pressure distortion Distortion screen Flow distortion	Unclassified - unlimited STAR Category 07

19. Security Classif. (of this report)	20. Security Classif. (of this page)	21. No. of Pages	22. Price*
Unclassified	Unclassified	39	$4.00

* For sale by the National Technical Information Service, Springfield, Virginia 22161

ERRATA

NASA Technical Memorandum X-3446

INTERNAL FLOW CHARACTERISTICS OF A MULTISTAGE COMPRESSOR WITH INLET PRESSURE DISTORTION

Claude E. deBogdan, John E. Moss, Jr., and
Willis M. Braithwaite

February 1977

Page 5, lines 14, 16, and 17: The word "temperature" should be replaced with the word "pressure."

Issued April 1977

INTERNAL FLOW CHARACTERISTICS OF A MULTISTAGE COMPRESSOR WITH INLET PRESSURE DISTORTION

by Claude E. deBogdan, John E. Moss, Jr.,
and Willis M. Braithwaite

Lewis Research Center

SUMMARY

The measured distribution of compressor interstage pressures and temperatures resulting from a 180° inlet-total-pressure distortion for a J85-13 turbojet engine are reported. Extensive inner stage instrumentation combined with stepwise rotation of the inlet distortion gave data of high circumferential resolution. The steady-state pressures and temperatures along with the amplitude, extent, and location of the distorted areas are given. Data are presented for 80, 90, and 100 percent of design rotor speed. These data are compared with clean (undistorted) inlet flow conditions and are plotted to show pressure and temperature behavior within the compressor. Results show that both overall and stagewise compressor performances vary only slightly when clean and distorted inlet conditions are compared. Total- and static-pressure distortions increase in amplitude in the first few stages of the compressor and then attenuate fairly uniformly to zero at the discharge. Total-temperature distortion induced by the pressure distortion reached a maximum amplitude by the first two stages and decayed only a little through the rest of the compressor. Distortion amplitude tended to peak in line with the screen edges and, except for total and static pressure in the tip zone, there was little swirl in the axial direction. Detailed distortion profiles for each station are given in the appendix.

INTRODUCTION

The J85-13 turbojet engine tests measured compressor internal temperatures and pressures resulting from a 180° of extent inlet pressure distortion. Such

measurements are needed to develop and validate analytical models that adequately predict engine performance and stability under distorted-inlet conditions. The availability of these models will reduce the need for much expensive and time consuming full-scale engine testing. Previous tests (refs. 1 and 2) have considered only overall performance with instrumentation being limited mainly to inlet and exit of the compressor and turbine. These tests have required many engine runs with many different circumferential and radial distortion patterns. The empirical distortion indexes that resulted from these tests were only applicable to specific engine designs.

A more successful attempt at predicting the effects of inlet-flow distortion has used a simplified parallel compressor model (refs. 3 to 5). However, the success has been limited to simple compressors with 60° or greater circumferential inlet distortions. The model is not detailed enough to handle the type of distortion encountered in flight or the more complex engines of today. More detailed models are being developed that use stage by stage compressor characteristics instead of the overall values used in the parallel compressor method. To validate these more detailed models, it is necessary to measure the compressor's internal temperatures and pressures resulting from inlet-flow distortion. Such data were obtained for the TF30-P3 turbofan engine (refs. 6 and 7) and were used to build the analytical model of reference 8. The experimental measurements of this report are being used to confirm another analytical model being developed for the J85-13 turbojet engine (ref. 9).

Circumferential profiles of both total pressure and total temperature were measured at hub, mean, and tip portions of each of the eight-stage stator passages. A technique for increasing the resolution of the circumferential profiles by rotating the distortion is described in reference 7. This technique was used in obtaining the data in this report. Circumferential static-pressure profiles were obtained at the outer wall for each of the eight stators and at the hub for stators 1 and 2. The data were collected for 80, 90, and 100 percent of rotor design speeds at a Reynolds number index of 0.7. The data have been reduced to give figures showing (1) a comparison of the overall performance of the engine with and without inlet distortion, (2) the degree and distribution of temperature distortion buildup resulting from pressure distortion, (3) the relative amplitude, extent, and distribution of the distorted pressure and temperature areas as they move through the compressor, (4)

the effect of speed on the swirl and extent of the distorted areas, and (5) the stage by stage maximum amplitude of pressure and temperature distortion.

Individual stage distortion profiles are given in the appendix. One complete set for hub, tip, and mean is given for 100 percent speed, but for the 90 and 80 percent speeds only tip static pressure and mean total pressure and total temperature are shown.

APPARATUS AND PROCEDURE

Engine

The J85-13 engine used for this test is a single-spool turbojet with an eight stage axial compressor, and a two stage turbine. Its inlet guide vanes (IGV's) are variable and are mechanically linked to compressor bleed valves so that, when the bleeds are fully open, the IGV's are fully closed. The bleeds are scheduled linearly from fully open at 80 percent of design rotor speed to fully shut at 94 percent of design rotor speed. This same engine was used for the stall margin tests of reference 10. A photograph of a typical installation of a J85-13 engine installed in the altitude chamber is given in figure 1.

Distortion Screens

The inlet-total-pressure distortion was generated with a screen located approximately 46 centimeters ahead of the IGV. The distortion screen had a square grid of 0.081-centimeter-diameter wire, spaced 0.282 centimeter apart (porosity = 0.51) and covered 180° of the compressor inlet.

Instrumentation

Compressor-face instrumentation at station 2.0 consisted of an array of 55 total-pressure probes arranged in 11 rakes of 5 probes each, a 10 probe boundary-layer rake, 20 total-temperature probes in 4 rakes of 5 probes each, and 4 tip and 1 hub static-pressure tap. The total-pressure probes were arranged to measure pressure in zones of equal area. Each compressor stage had a total-pressure rake and a total-temperature rake in its stator passages. Each rake had three probes (tip, mean,

and hub). There were also a wall static-pressure tap at the trailing-edge region of each stator and wall static taps in the hub regions of the first and second stators. A layout of the instrumentation at each station is shown in figure 2; radial, axial, and circumferential locations for the probes are listed in table I.

Procedure

The amounts of instrumentation that can be placed in a compressor is limited by the available space. Adequate circumferential coverage is especially difficult to achieve. Each rake partially blocks the stator passage and thus affects the flow. Therefore, it is desirable to minimize the number of rakes per stage. To compensate for the problem of inadequate circumferential instrumentation, the distortion screen was rotated a full circle in thirty-six 10° steps, one step per run. This had the effect of multiplying the instrumentation thirty-six-fold.

The engine was initially set up with the 180° distortion screen alined with the 0 to 180° sector of the engine face. Data were taken at 80, 90, and 100 percent of design rotor speed and a Reynolds number index of 0.7. The screen was then manually rotated 10° counterclockwise and another three runs were made. (Throughout this report all references to circumferential position or direction are given as if one were aft of the engine and looking forward.) This procedure was repeated 35 times to complete a full circle. In plotting a 36-run set of data for a given rotor speed and rake, the point for the first run (screen in the 0 to 180° position) was plotted on the abscissa at the circumferential position of the rake. The point for the second run was plotted 10° clockwise (opposite to screen rotation) and so on. Relatively speaking, this procedure is equivalent to holding the screen fixed and rotating the instrumentation. Data were corrected to upstream plenum pressures and temperatures in order to compensate for run to run variations.

RESULTS

Distortion

Ring average values (average of 36 runs for each hub, tip, and mean probe) for static pressure, total pressure, and total temperature are given in table II. Ten static taps were located in the inlet duct to measure the variation in static-pressure distortion between the distortion screen and station 2.0. Figure 3 shows this variation for 90 and 100 percent of design rotor speed. The behavior of static pressure for both rotor speeds is similar. Ample opportunity for crossflow causes the distortion (at 100 percent of design rotor speed, for example) to decay in amplitude from 0.80 to 0.56 as it moves from 8 to 22 centimeters downstream of the screen. However, the pumping action of the engine reverses this trend approximately 14 centimeters upstream of station 2.0, and static pressure builds up rapidly near the inlet guide vanes.

Figure 4 shows that the total-temperature distortion at station 2.0 is a fairly uniform square wave with minor disturbances due to screen support struts. The static-pressure profile is in phase with total temperature but is sinusoidal with an amplitude about one-half that of the total-temperature distortion. The broadness of both curves in this figure is due to data scatter in that the data of 11 probes (one for each rake) are overplotted for total temperature and 5 taps are overplotted for static pressure. Total-temperature input distortion (not shown) is essentially zero.

Compressor Average Performance

The effect of distortion on overall compressor performance is given in figure 5. Here, overall pressure and temperature ratios are plotted against speed for both distorted and clean (not distorted) inlets. No significant difference can be seen except for a very slight decrease in pressure ratio at 100 percent of design rotor speed. There is, however, a noticeable decrease in weight flow with distortion (fig. 5(c)). This decrease is consistant with the results of reference 1.

A more detailed look at the difference between distorted and clean-inlet performance is shown in figure 6. In this series of plots the performance of each stage is plotted against stage number. Here again, where average values are concerned,

the distorted inlet causes little degradation in performance. The slight deviation in the total-pressure rise per stage from the clean inlet condition is greatest at high speed and near the hub for the first three stages. There is almost no difference from stage 4 through the compressor exit. The deviation of total-temperature rise follows the same pattern of small deviations as for the total-pressure rise, but with a little more scatter throughout the compressor, particularly at the hub at 100 percent speed.

Since there is almost no difference between clean and distorted overall performance, the average lines of figure 4 represent the clean-inlet data. The pressure and temperature profiles deviate above and below the clean-inlet condition instead of being generally depressed. This condition holds throughout the compressor as can be seen in the appendix figures.

Internal Distortions

Figure 7 is a series of plots of distortion amplitude versus relative circumferential position for 100-percent of rotor design speed. The stage plots are arranged so one can easily see the variation in amplitude, rotation, and decay of distortion as it moves through the compressor. The definition of amplitude for this figure and the appendix figures is the same, that is, P/P_{av}. The sinusoidal static-pressure distortion input at station 2.0 is immediately amplified and rotated counterclockwise at station 2.1. The shape and position at station 2.2 is similar but of slightly lower amplitude. Distortion at both 2.1 and 2.2 is concentrated at a position in line with the leading edge (0) of the distortion screen. While there is about a 90° counterclockwise shift in the full extent of the distortion for these stages, the majority of the distorted area is still located at a peak just past the leading edge of the screen. At station 2.3 the area has shifted back close to the original position coincident with the screen, with the peak remaining at the edge of the screen. For the rest of the compressor the peak disappears, and distortion amplitude diminishes until it is unmeasurable at station 3.0.

The plot of tip total pressure (fig. 7(d)) is almost identical to the tip static plot of figure 7(a). Amplitude span and location of the distorted areas agree almost everywhere but at station 2.3. At that station there is a low-amplitude static-pressure distortion from 110° to 180° that does not appear for total-temperature dis-

tortion. The peak areas at 2.3 do agree, however. The similarity of figure 7(a) and (d) implies a constant circumferential total to static ratio, which indicates a uniform Mach number throughout the tip zone. The mean and hub plots of figure 7 show less swirl. The front stages again concentrate the distortion at the leading edge of the screen. The mean zone has a tendency to shift the distortion to the trailing edge of the screen in the center stages of the compressor. Distortion has been attenuated to nearly zero at the final stage in the hub, mean, and tip zones.

Total-temperature distortion is shown in figures 7(e) to (g). Here, distortion is defined as any temperature greater than average. Distortion in the tip, mean, and hub rapidly builds up at the front of the compressor and is fully developed by station 2.2. The right edge of the distorted area remains fixed at about 45° clockwise of the screen trailing edge. This is so (within 10°) from the beginning to the end of the compressor and for all three zones. The left edge position for the hub remains at 90° with some very low amplitude extension counterclockwise of 90° at stations 2.1 and 2.2. The left boundary for the mean zone remains at about 150° leaving a distorted area of only 75° to 80° of extent. The left boundary of the tip distortion tends to shift in low amplitude counterclockwise. All three zones have the majority of the distorted area located clockwise of the screen trailing edge by about 10°. Peaking is most evident in the mean zone and least evident in the hub. At station 3.0 the tip, mean, and hub show the distorted region to be spreading counterclockwise, and all three areas have about the same extent of distortion amplitude and position.

The effect of speed can be seen by comparing figures 7 and 8. In figure 8 the tip static pressure and mean total pressure and temperature distributions at 80 percent of rotor design speed are plotted. These patterns are essentially consistent with those shown for the 100-percent-speed condition except for diminished amplitude and much less peaking.

The manner in which static-pressure, total-pressure, and total-temperature distortions vary axialy through the compressor is given for all three speeds in figure 9. The distortion in these plots is defined as (maximum - minimum)/average and is calculated from the circumferential profile plots of the appendix. The three plots are similar, differing only in amplitude. The static- and total-pressure distortions reach a maximum by stage 1. Static pressure distortion attenuates fairly uniformly to almost zero at stage 8. Total pressure is not attenuated significantly until stage 4. Beyond that stage total pressure distortion falls off uniformly until it is zero at stage

8. Total temperature distortion reaches a maximum amplitude by stage 2, remains fairly constant back to stage 5, and then falls slightly for the rest of the compressor.

SUMMARY OF RESULTS

1. The 180° distortion screen produced a well defined square wave in total pressure at station 2.0.

2. Static-pressure distortion created by the screen decays for the first 22 centimeters of the path from screen to compressor inlet. It then begins to rise, because of the pumping action of the compressor. The resulting sinusoidally shaped static-pressure distortion has an amplitude of about one half the total-pressure distortion at station 2.0.

3. The distorted and clean inlet overall and stagewise compressor performance are essentially the same.

4. There is an abrupt 90° counterclockwise (looking upstream) rotation of static-pressure distortion at stations 2.1 and 2.2 which is reversed at station 2.3.

5. Both tip total- and static-pressure distortions peak at a position in line with the edge of the screen until the rear of the compressor where they even out and decrease to zero.

6. Total- and static-pressure distortions in the tip zone are almost identical throughout the compressor, which indicates a circumferentially constant Mach number.

7. Hub and mean zones of total-pressure distortion show little rotation, while distortion at the tip shows the same abrupt 90° counterclockwise shift as for static pressure.

8. The static- and total-pressure distortions increase in the first few compressor stages and are then attenuated uniformly to a value of approximately zero at stage 8. Both distortions generally attenuate after this stage, becoming less than 1 percent at the compressor exit.

9. A total-temperature distortion is generated in the first two stages and is concentrated in a line with the trailing edge of the screen. The amplitude decays only slightly throughout the compressor.

9. A total-temperature distortion is generated in the first two stages and is concentrated in a line with the trailing edge of the screen. The amplitude decays only slightly throughout the compressor.

Lewis Research Center,
National Aeronautics and Space Administration,
Cleveland, Ohio, August 16, 1976,
505-05.

REFERENCES

1. Calogeras, James E.; Mehalic, Charles M; and Burstadt, Paul L.: Experimental Investigation of the Effect of Screen-Induced Total-Pressure Distortion on Turbojet Stall Margin. NASA TM X-2239, 1974.

2. Mehalic, Charles M.; and Lottig, Roy A.: Steady-State Inlet Temperature Distortion Effects on the Stall Limit of a J85-GE-13 Turbojet Engine. NASA TM X-2990, 1974.

3. Graber, E. J., Jr.; and Braithwaite, W. M.: Summary of Recent Investigations of Inlet Flow Distortion Effects on Engine Stability. AIAA Paper 74-236, Feb. 1974.

4. Braithwaite, W. M.; Graber, E. J., Jr.; and Mehalic, C. M.: The Effects of Inlet Temperature and Pressure Distortion on Turbojet Performance. AIAA Paper 73-1316, Nov. 1973.

5. Proceedings of the NASA Conference on Aeronautical Propulsion. SP-381, 1975.

6. Evans, David G.; et al.: Some Comparisons of the Flow Characteristics of a Turbofan Compressor System With and Without Inlet Pressure Distortion. NASA TM X-71574, 1974.

7. deBogdan, Claude E., et al.: Effect of a 180°-Extent Inlet Pressure Distortion on the Internal Flow Conditions of a TF30-P-3 Engine. NASA TM X-3267, 1975.

8. Mazzawy, R. S.; and Banks, G. A.: Modeling and Analysis of the TF30-P-3 Compressor System with Inlet Pressure Distortion. (PWA-5302, Pratt & Whitney Aircraft; NAS3-18535) NASA CR-134996, 1976.

9. Tesch, W. A.; and Steenken, W. G.: Blade Row Dynamic Digital Compressor Program. Vol. 1: J85 Clean Inlet Flow and Parallel Compressor Models. (R75AEG406, General Electric Co.; NAS3-18526) NASA CR-134978, 1976.

10. Wenzel, Leon M.; Moss, John E., Jr.; and Mehalic, Charles M.: Effect of Casing Treatment on Performance of a Multistage Compressor. NASA TM X-3175, 1975.

TABLE I. - INSTRUMENTATION LOCATION

Station	Instrumentation		Circumferential position, deg	Radial position		Axial distance from inlet guide vane, cm
	Type (a)	Position		cm	Percent of passage height	
1.01	PS	Tip	60	20.4	100	-37.8
1.02						-35.9
1.03						-34.0
1.04						-32.1
1.05						-30.2
1.06						-28.3
1.07						-26.4
1.08						-24.5
1.09						-22.6
1.10						-20.7
2.0	PS	Tip	60	20.4	100	-9.8
			120	↓	↓	↓
			240			
			300			
		Hub	90	5.8	0	-6.9
	PT[b]	Tip	15	19.4	95	-6.9
		Mean	15	14.9	73	-6.9
		Hub	15	8.0	39	-12.3
	TT[c]	Tip	30	18.7	91	↓
		Mean	30	14.8	72	
		Hub	30	11.7	57	
2.1	PS	Tip	128	19.9	100	14.0
			293	19.9	100	14.0
		Hub	315	11.1	0	14.0
	PT	Tip	136	19.1	90	11.9
		Mean	136	15.5	50	↓
		Hub	136	11.9	10	
	TT	Tip	158	19.1	90	
		Mean	158	15.5	50	
		Hub	158	11.9	10	
2.2	PS	Tip	115	19.7	100	17.9
			295	19.7	100	17.9
		Hub	315	12.9	0	17.9
	PT	Tip	136	19.0	90	16.7
		Mean	136	16.3	50	↓
		Hub	136	13.6	10	
	TT	Tip	155	19.0	90	
		Mean	155	16.3	50	
		Hub	155	13.6	10	
2.3	PS	Tip	116	19.7	100	21.6
			296	19.7	100	21.6
	PT		131	19.2	90	20.4
		Mean	131	17.1	50	↓
		Hub	131	14.9	10	
	TT	Tip	153	19.2	90	
		Mean	153	17.1	50	
		Hub	153	14.5	10	
2.4	PS	Tip	117	19.7	100	24.6
			297	19.7	100	24.6
	PT		130	19.3	90	23.7
		Mean	130	17.6	50	↓
		Hub	130	15.9	10	
	TT	Tip	150	19.3	90	
		Mean	150	17.6	50	
		Hub	150	15.9	10	
2.5	PS	Tip	117	19.7	100	27.7
			298	19.7	100	27.7
	Pt	Tip	127	19.3	90	26.4
		Mean	127	17.9	50	↓
		Hub	127	16.6	10	
	TT	Tip	147	19.3	90	
		Mean	147	17.9	50	
		Hub	147	16.6	10	
2.6	PS	Tip	117	19.7	100	30.1
			298	19.7	100	30.1
	PT	Tip	127	19.4	90	29.1
		Mean	127	18.2	50	↓
		Hub	127	16.9	10	
	TT	Tip	147	19.4	90	
		Mean	147	18.2	50	
		Hub	147	16.9	10	
2.7	PS	Tip	117	19.7	100	32.5
			299	19.7	100	32.5
	PT	Tip	127	19.1	90	31.2
		Mean	127	18.3	50	↓
		Hub	127	17.1	10	
	TT	Tip	147	19.4	90	
		Mean	147	18.3	50	
		Hub	147	17.1	10	
2.8	PS	Tip	106	9.7	100	34.7
			298	9.7	100	34.7
3.0	PS	Tip	[d]30	19.7	100	39.9
	PT	Tip	↓	19.3	93	↓
		Mean		18.7	79	
		Hub		18.1	66	
	TT	Tip		19.3	93	
		Mean		18.7	79	
		Hub		18.1	66	

[a] PS = static-pressure tap; PT = total pressure probe; TT = total temperature probe.
[b] Repeated every 30° except at 285°.
[c] Repeated at 150°, 210°, and 330°.
[d] PS, PT, and TT arrangement repeated at 150°, 210°, and 330°.

TABLE II. - RING AVERAGE VALUES OF STATIC PRESSURE, TOTAL PRESSURE, AND TOTAL TEMPERATURE

Station	Percent speed	Static pressure $P_{s'_2}$ N/cm^2		Total pressure, $P_{tot'_2}$ N/cm^2			Total temperature, $T_{tot'}$ K		
		Hub	Tip	Hub	Mean	Tip	Hub	Mean	Tip
2.0	100	5.166	5.153	5.949	5.958	5.896	274.05	274.23	274.57
	90	6.016	5.687	6.235	6.243	6.243	274.74	274.92	275.24
	80	6.028	6.019	6.397	6.406	6.345	275.37	275.52	275.88
2.1	100	6.259	6.402	8.211	8.665	8.740	304.89	308.47	317.61
	90	6.629	6.813	7.916	8.154	8.455	297.64	299.52	307.61
	80	6.340	6.527	7.268	7.407	7.587	288.74	288.29	293.78
2.2	100	8.677	9.525	8.502	11.576	12.334	340.36	342.09	351.95
	90	8.854	9.444	11.028	10.928	11.524	324.44	328.32	336.58
	80	8.005	8.336	9.377	9.473	9.779	308.46	311.98	318.61
2.3	100	-----	12.514	15.720	16.177	16.568	377.84	381.37	394.46
	90	-----	12.321	14.275	14.308	14.874	357.56	358.76	371.31
	80	-----	10.482	11.672	11.979	12.078	337.03	336.53	344.82
2.4	100	-----	17.468	20.296	21.387	21.339	------	422.16	437.84
	90	-----	15.874	18.005	18.448	18.789	------	392.69	405.67
	80	-----	12.735	14.017	14.656	14.666	------	360.39	369.72
2.5	100	-----	22.474	25.797	27.379	26.506	455.62	451.01	470.99
	90	-----	20.594	22.269	23.123	23.020	422.36	420.96	429.17
	80	-----	16.393	16.728	17.599	17.477	384.73	381.21	384.66
2.6	100	-----	27.685	31.209	32.735	30.915	479.67	478.09	------
	90	-----	24.341	26.341	27.770	27.082	443.42	441.94	------
	80	-----	18.401	19.427	20.627	20.504	402.52	400.22	------
2.7	100	-----	32.819	36.278	37.097	34.442	------	------	------
	90	-----	28.148	30.451	31.280	30.949	------	------	------
	80	-----	20.696	22.110	22.698	22.548	------	------	------
2.8	100	-----	37.778	------	------	------	------	------	------
	90	-----	31.868	------	------	------	------	------	------
	80	-----	22.858	------	------	------	------	------	------
3.0	100	-----	38.849	41.179	40.977	40.129	512.69	521.31	535.39
	90	-----	32.682	34.409	34.318	34.409	472.26	475.32	484.12
	80	-----	23.392	24.626	24.529	24.077	421.25	423.18	426.62

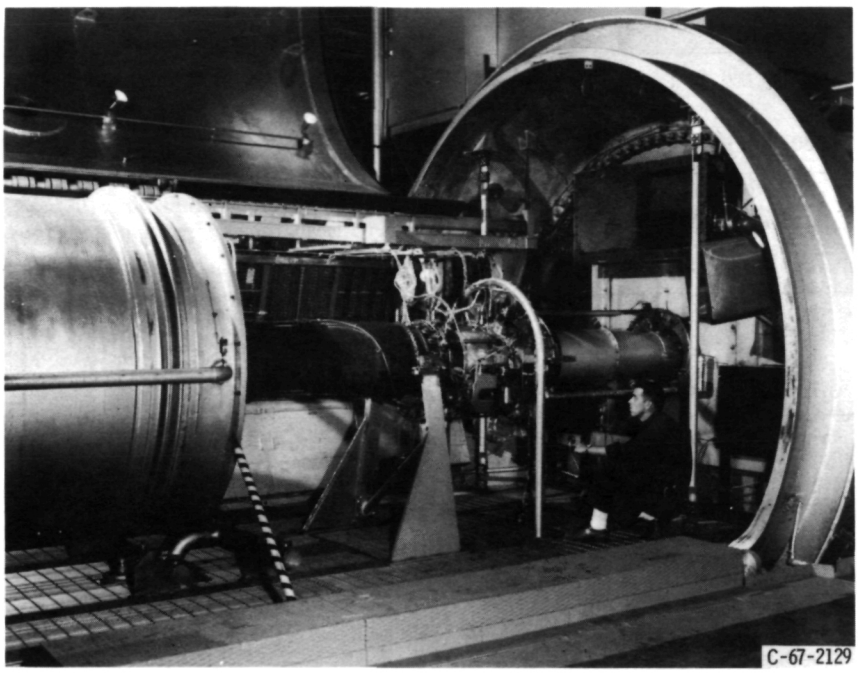

Figure 1. - Engine in tank.

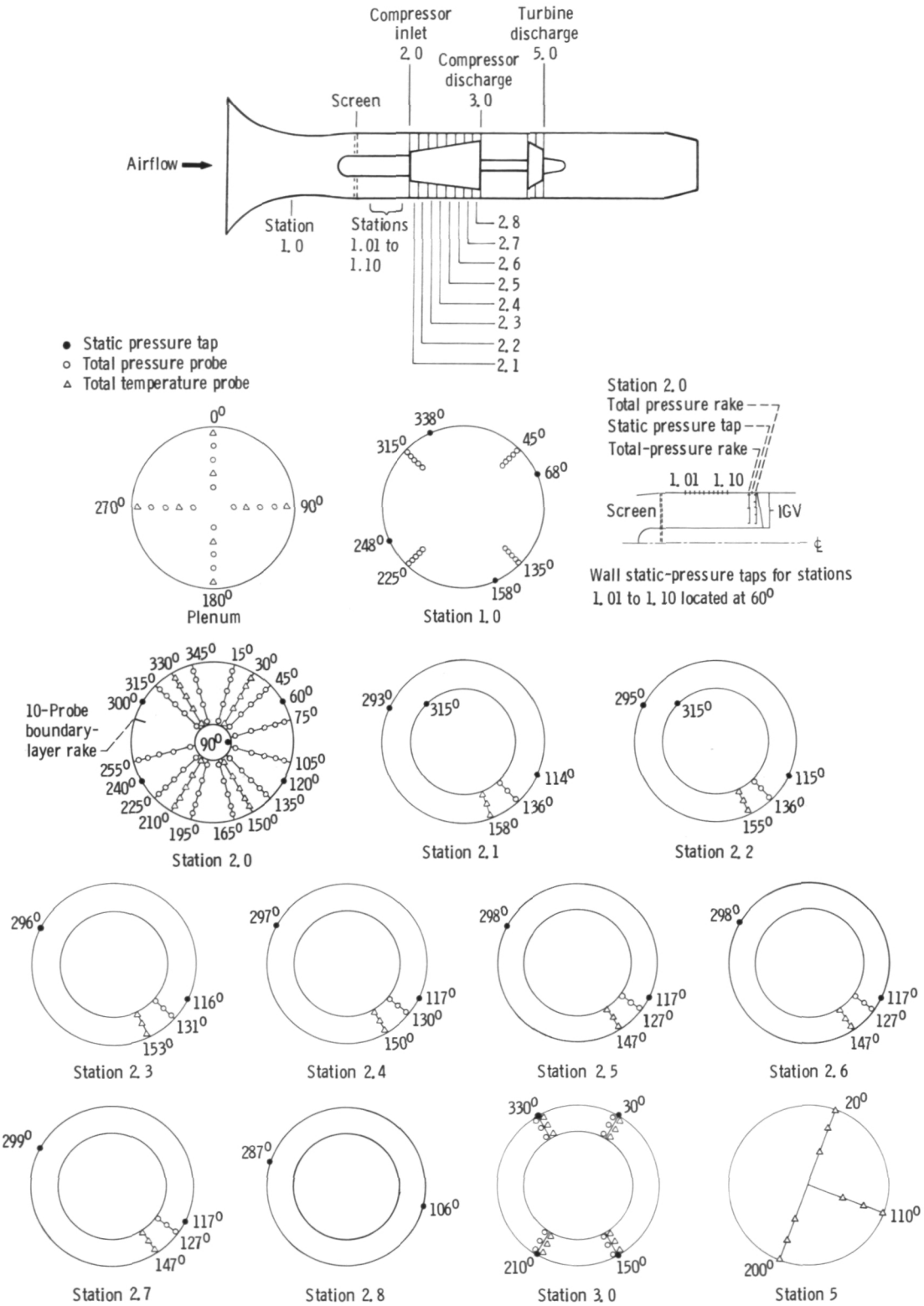

Figure 2. - Station schematic engine layout.

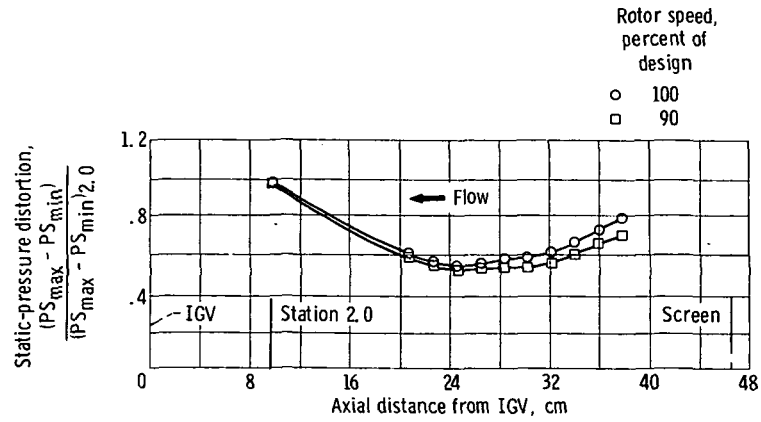

Figure 3. - Static-pressure distortion between inlet guide vane (IGV) and distortion screen.

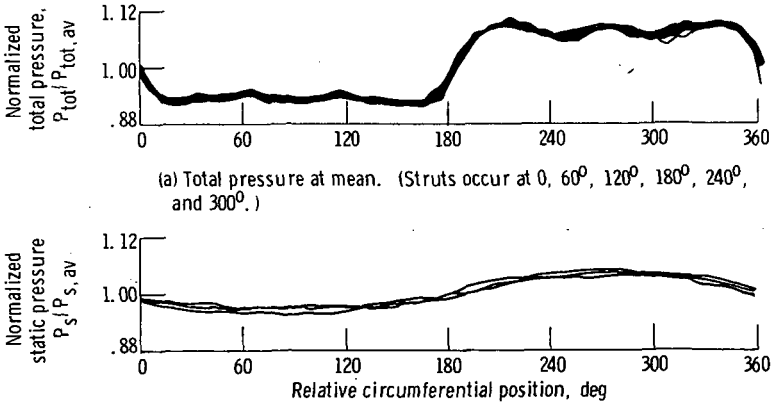

(a) Total pressure at mean. (Struts occur at 0, 60°, 120°, 180°, 240°, and 300°.)

(b) Static pressure at tip.

Figure 4. - Station 2.0 input distortion at 100 percent of design rotor speed.

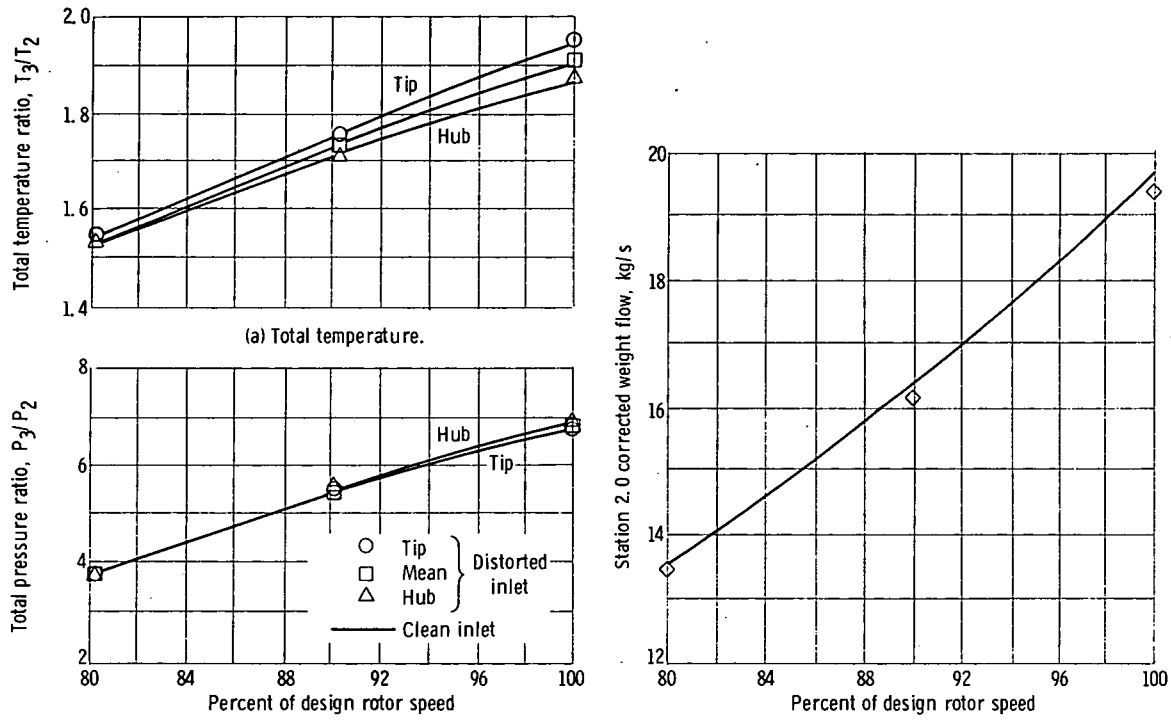

Figure 5. - Effect of distortion on overall compressor performance of J85-13 engine at 0.7 Reynolds number index.

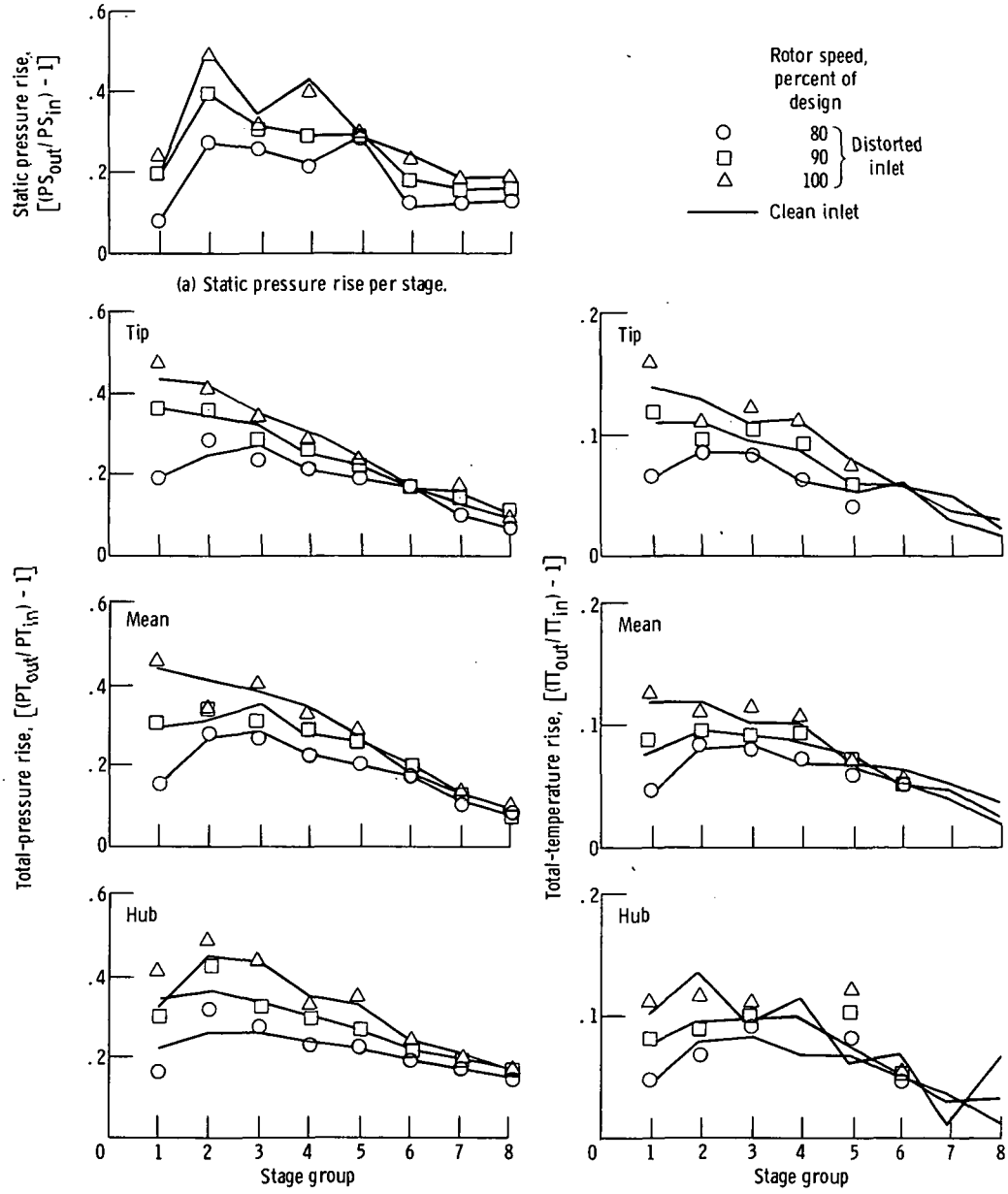

(a) Static pressure rise per stage.

(b) Total-pressure rise per stage.

(c) Total-temperature rise per stage.

Figure 6. - Comparison of distorted and clean inlet stage performance.

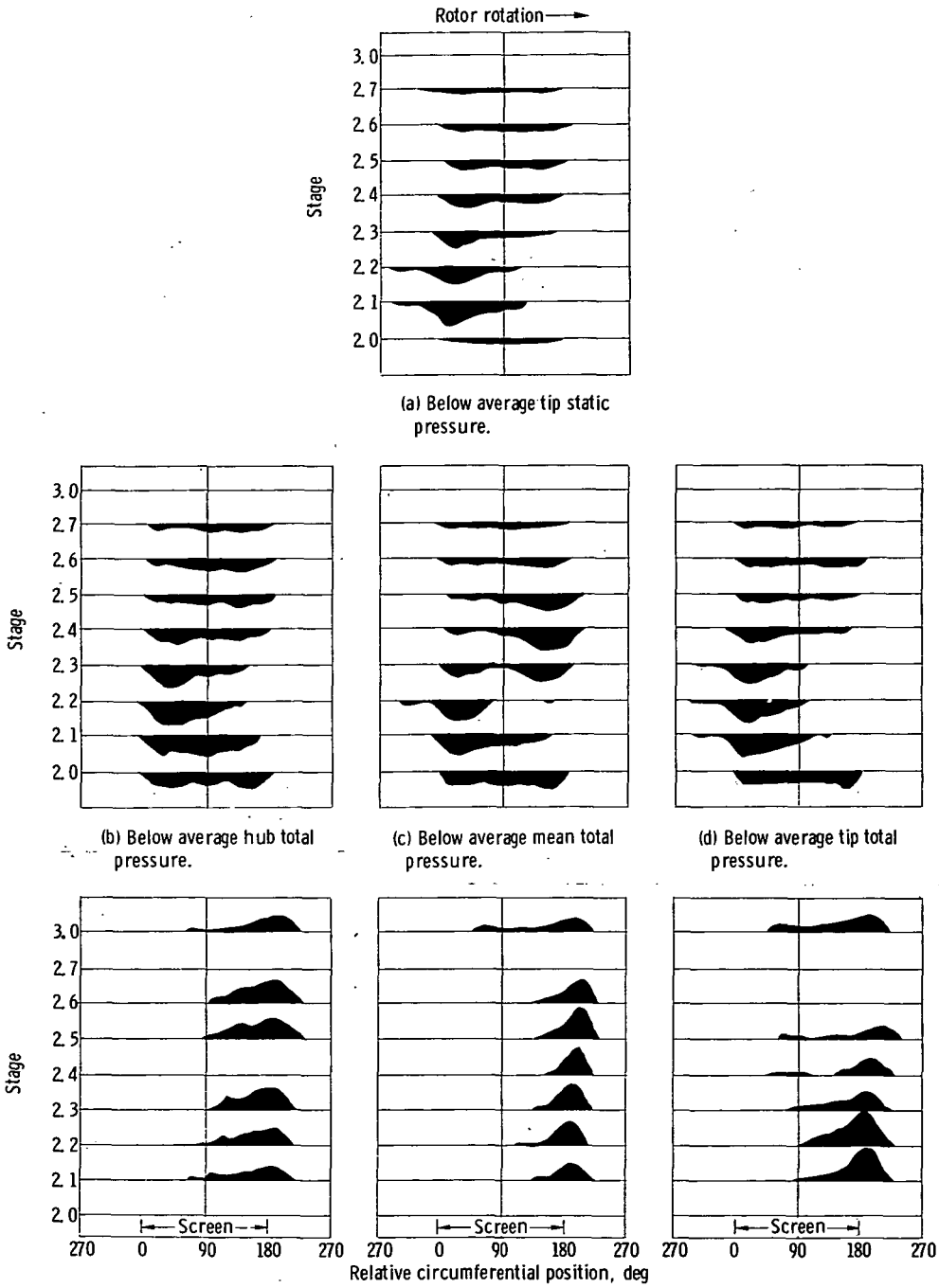

(a) Below average tip static pressure.

(b) Below average hub total pressure.

(c) Below average mean total pressure.

(d) Below average tip total pressure.

(e) Above average hub total temperature.

(f) Above average mean total temperature.

(g) Above average tip total temperature.

Figure 7. - Stage by stage relative circumferential position of distorted area at 100 percent of design rotor speed.

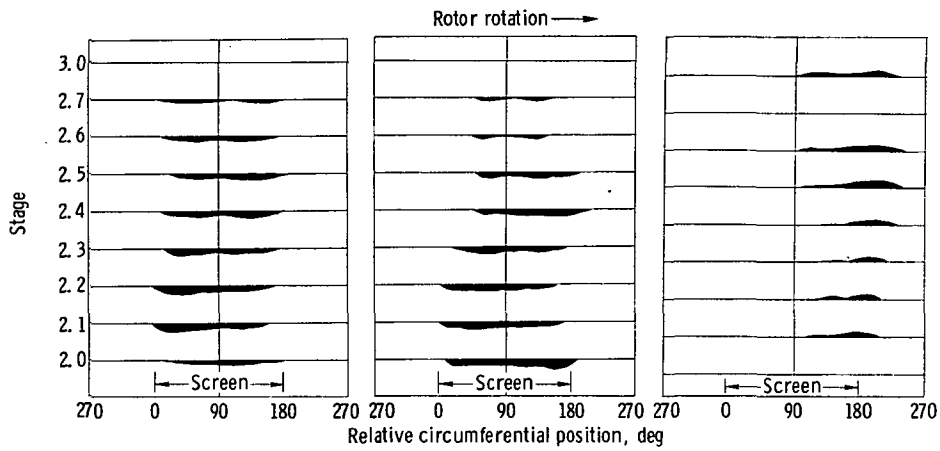

(a) Below average tip static pressure.

(b) Below average mean total pressure.

(c) Above average mean total temperature.

Figure 8. - Stage by stage relative circumferential position of distorted area at 80 percent of design rotor speed.

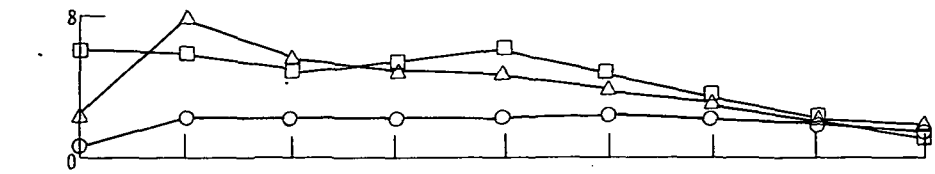

(a) Rotor speed, 80 percent of design.

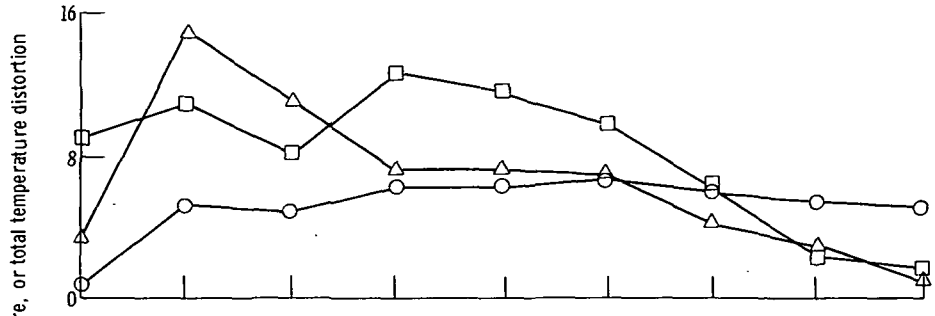

(b) Rotor speed, 90 percent of design.

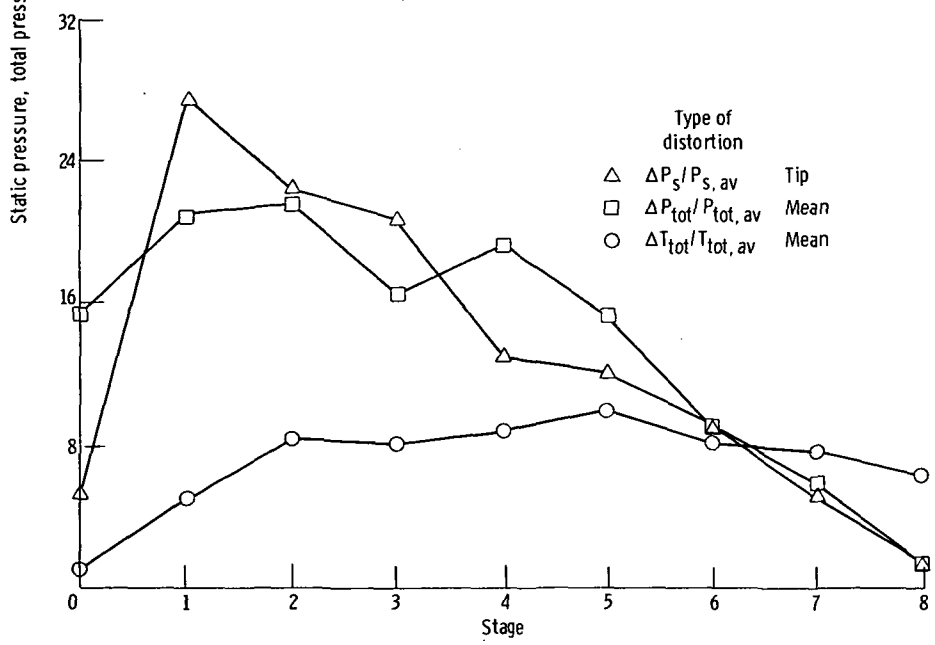

(c) Rotor speed, 100 percent of design.

Figure 9. - Internal distortion ((max - min)/av).

APPENDIX - CIRCUMFERENTIAL VARIATION IN STATIC PRESSURE, TOTAL PRESSURE, AND TOTAL TEMPERATURE

The basic rotated screen data taken for each of the three speeds are given in figures 10 to 14. The data are presented as probe values devided by the probe average and are plotted against relative circumferential position. Total and static pressures have been corrected for run to run deviations of the total pressure in the plenum from the average for all runs.

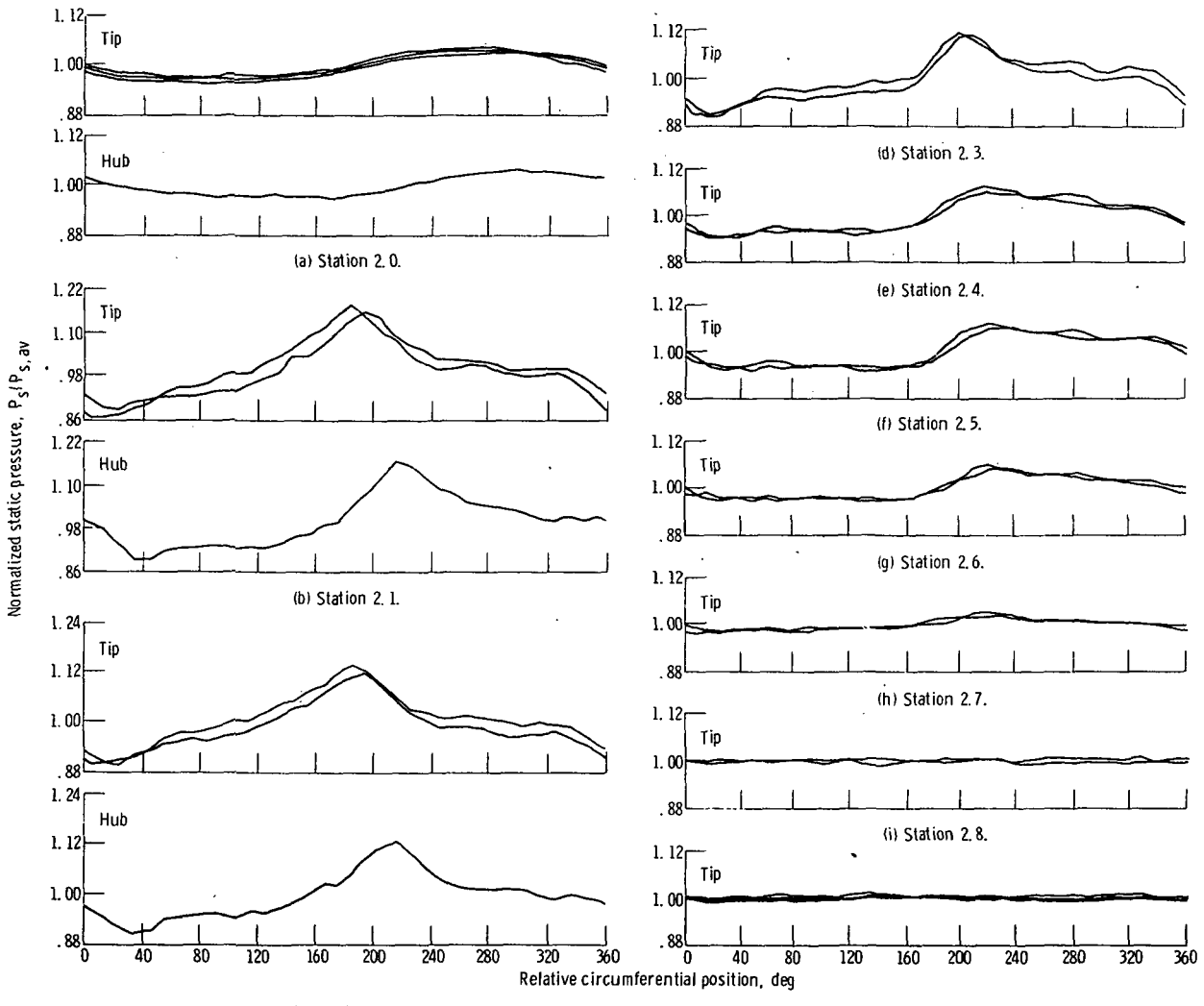

Figure 10. - Static-pressure profiles of distorted J85-13 inlet. Rotor speed, 100 percent of design.

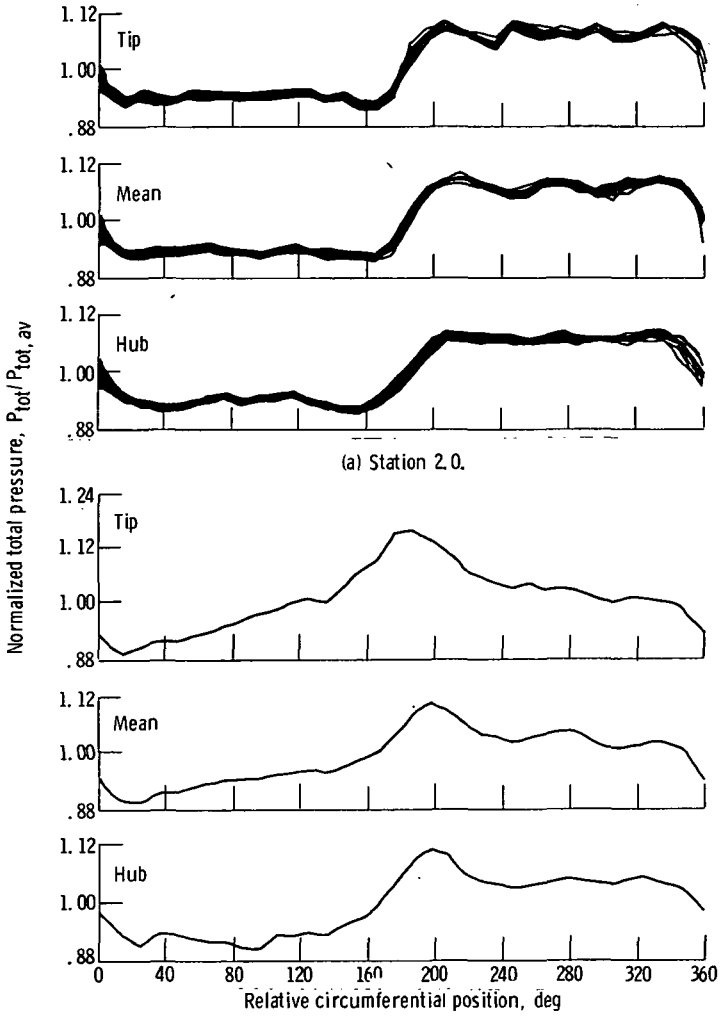

(a) Station 2.0.

(b) Station 2.1.

Figure 11. - Total pressure profiles for distorted J85-13 inlet. Rotor speed, 100 percent of design.

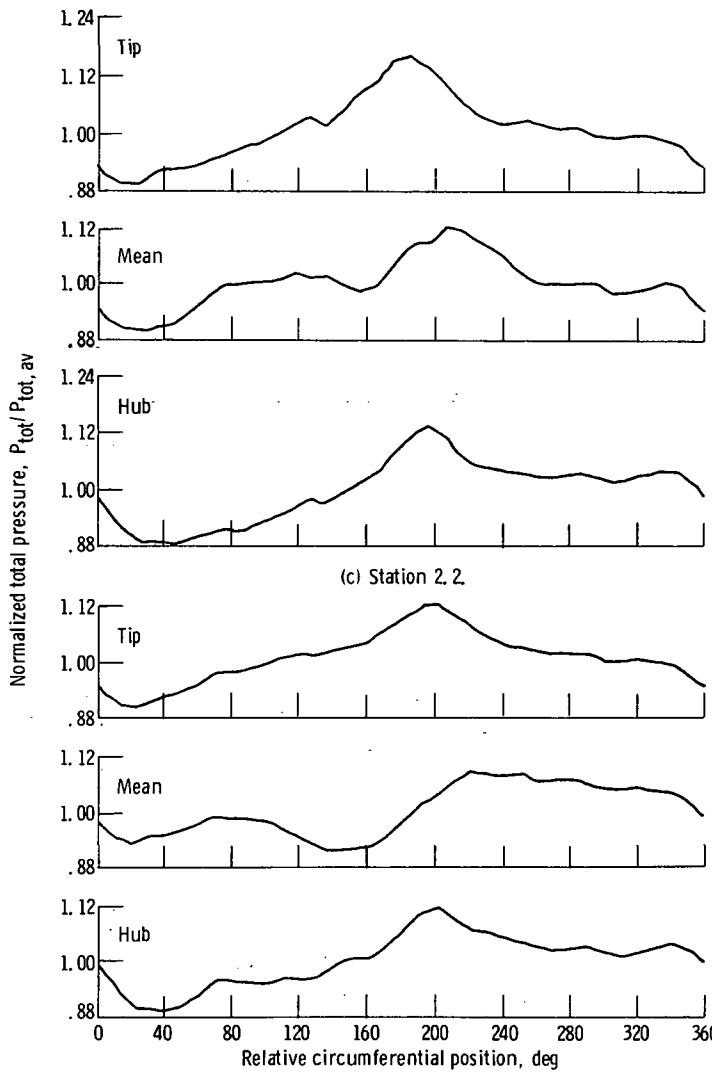

(c) Station 2.2.

(d) Station 2.3.

Figure 11. - Continued.

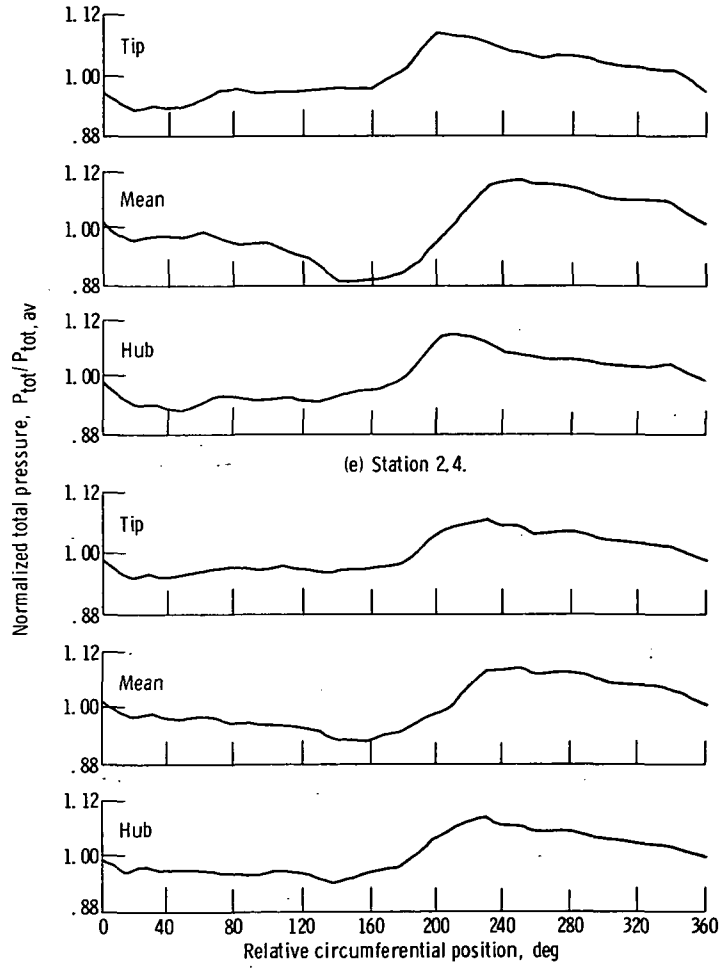

(e) Station 2.4.

(f) Station 2.5.

Figure 11. - Continued.

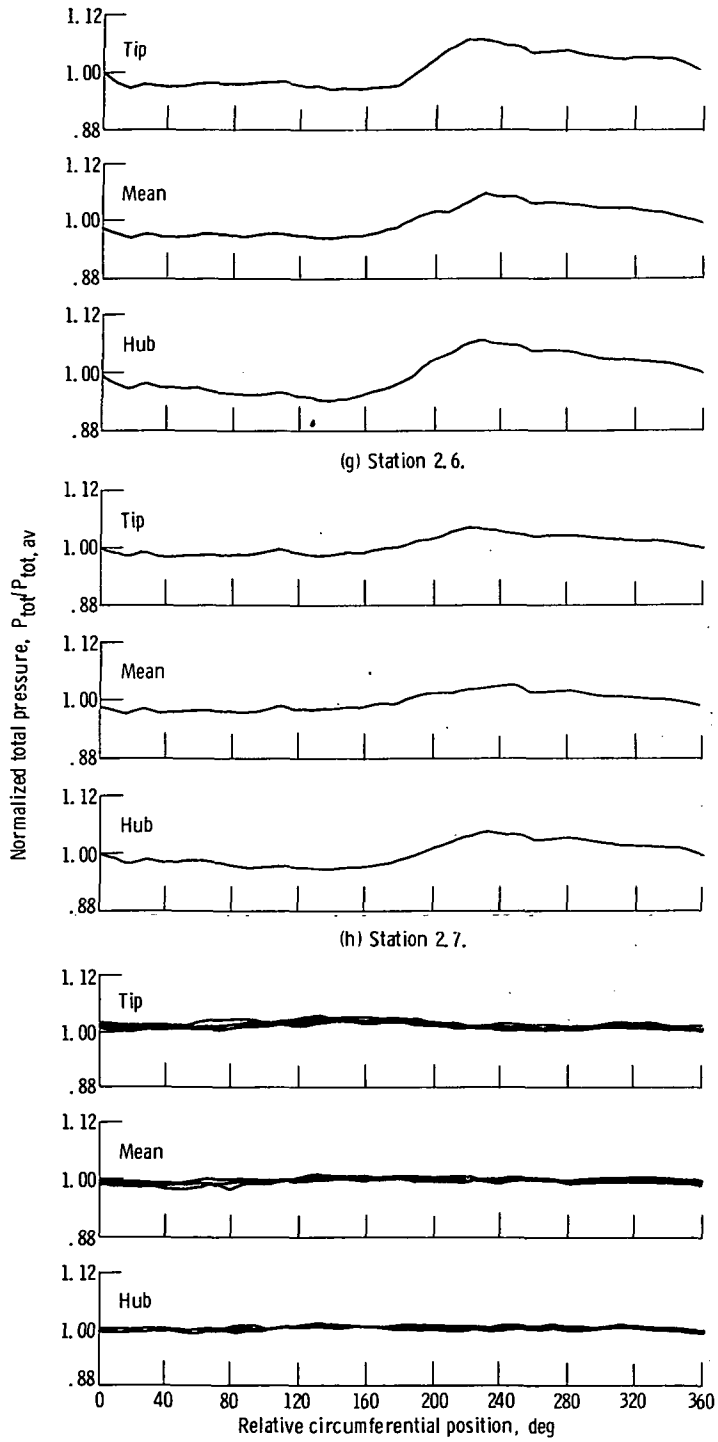

(g) Station 2.6.

(h) Station 2.7.

(i) Station 3.0.

Figure 11. - Concluded.

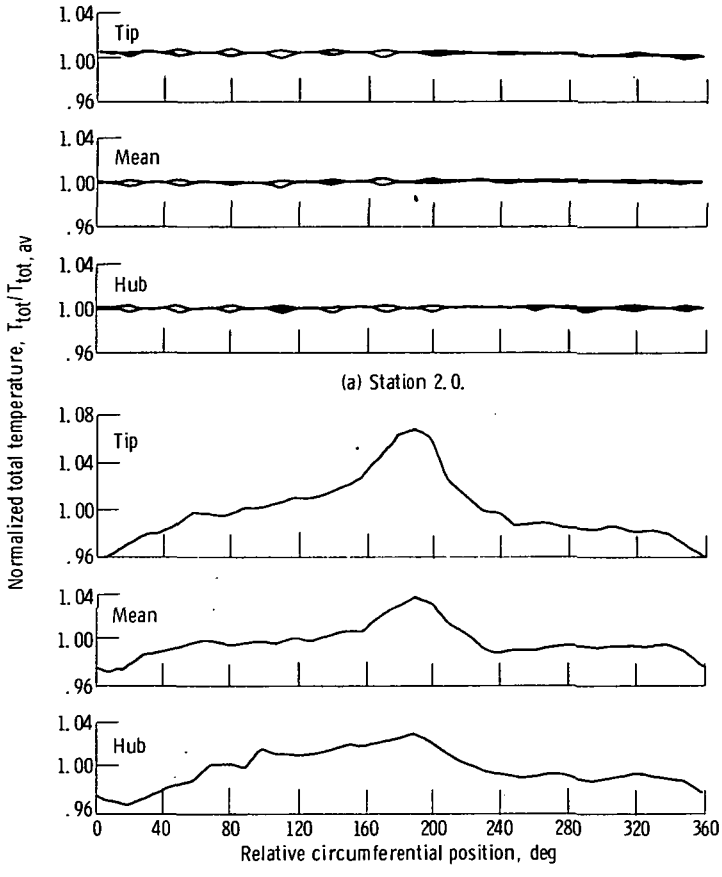

Figure 12. - Total temperature profiles for distorted J85-13 inlet. Rotor speed, 100 percent of design.

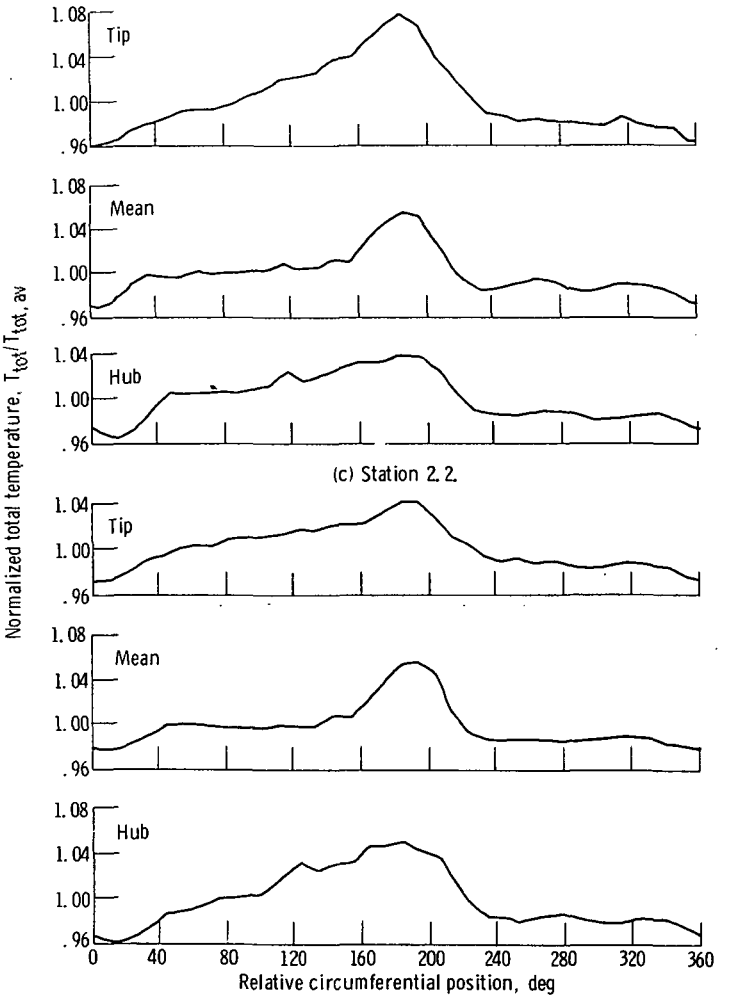

(c) Station 2.2.

(d) Station 2.3.

Figure 12. - Continued.

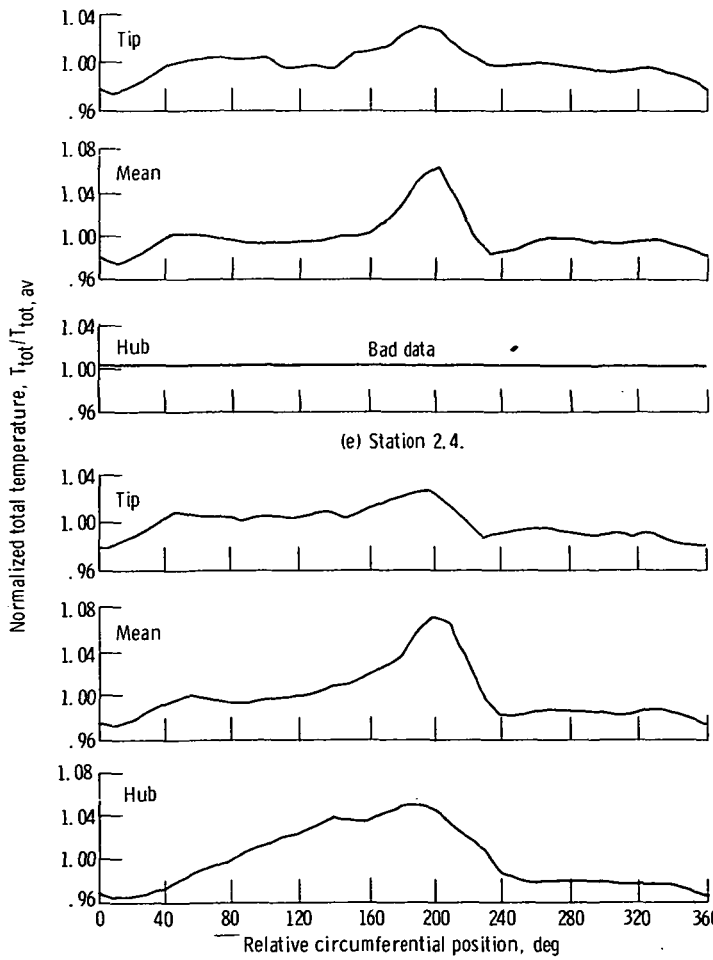

(e) Station 2.4.

(f) Station 2.5.

Figure 12. - Continued.

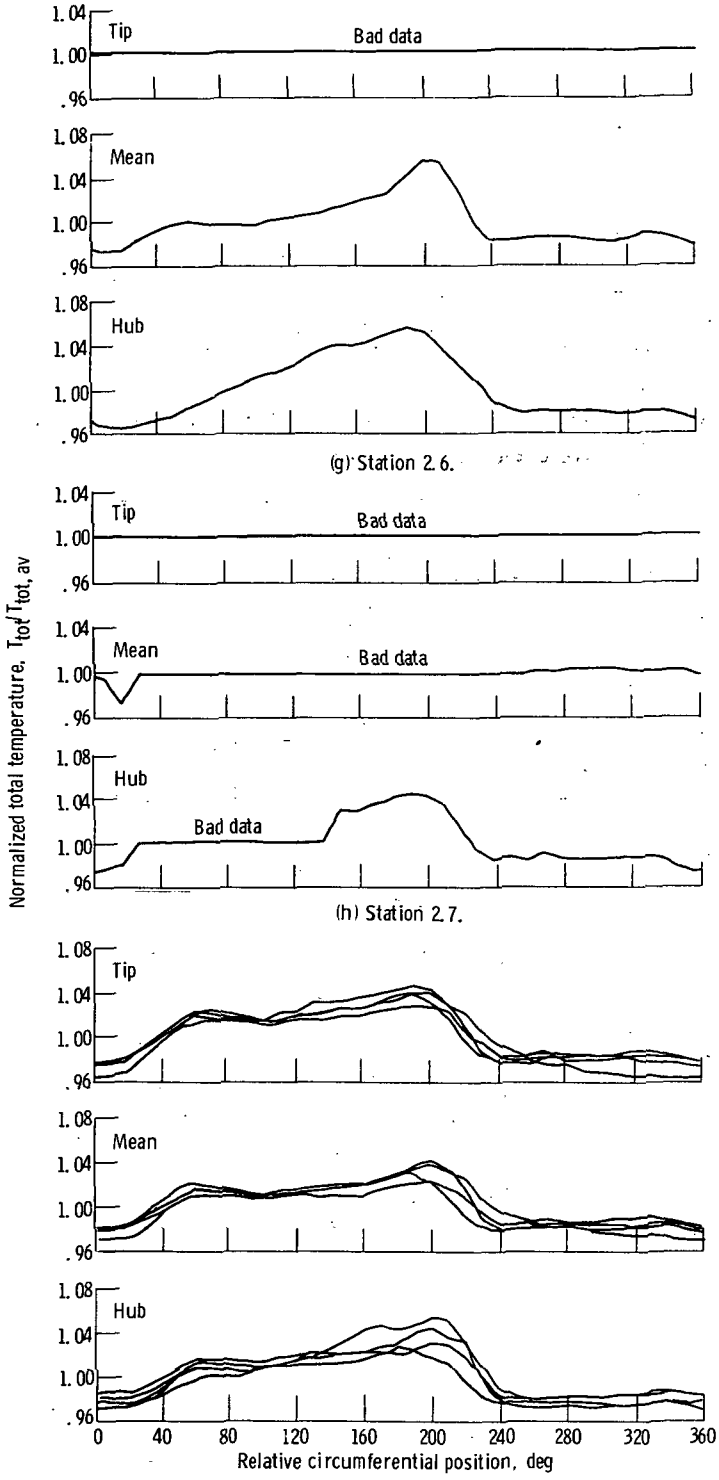

(g) Station 2.6.

(h) Station 2.7.

(i) Station 3.0.

Figure 12. - Concluded.

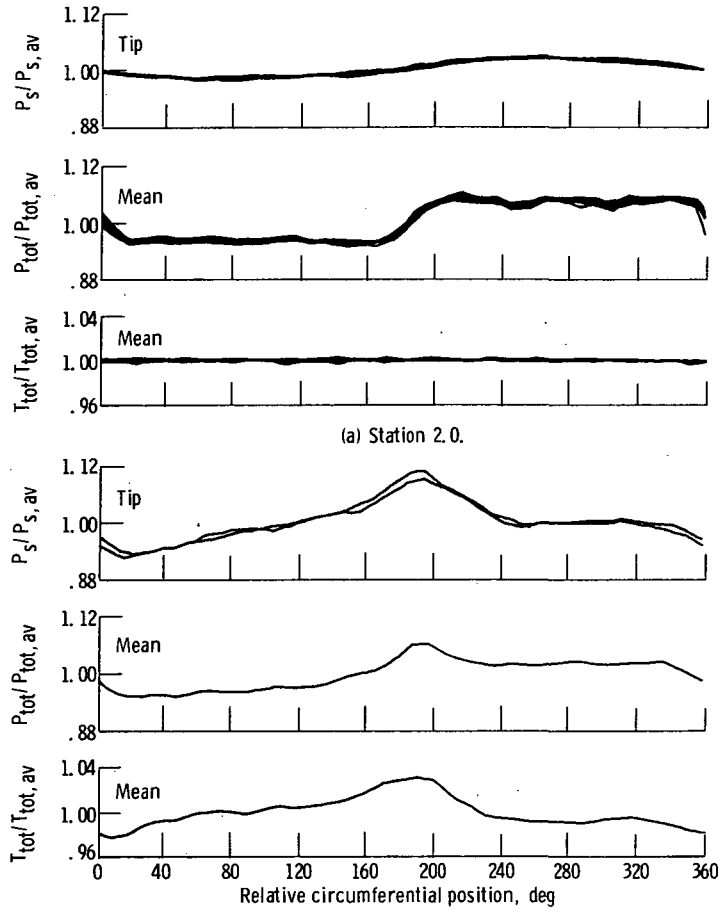

Figure 13. - Static- and total-pressure and total-temperature profiles for distorted J85-13 inlet. Rotor speed, 90 percent of design.

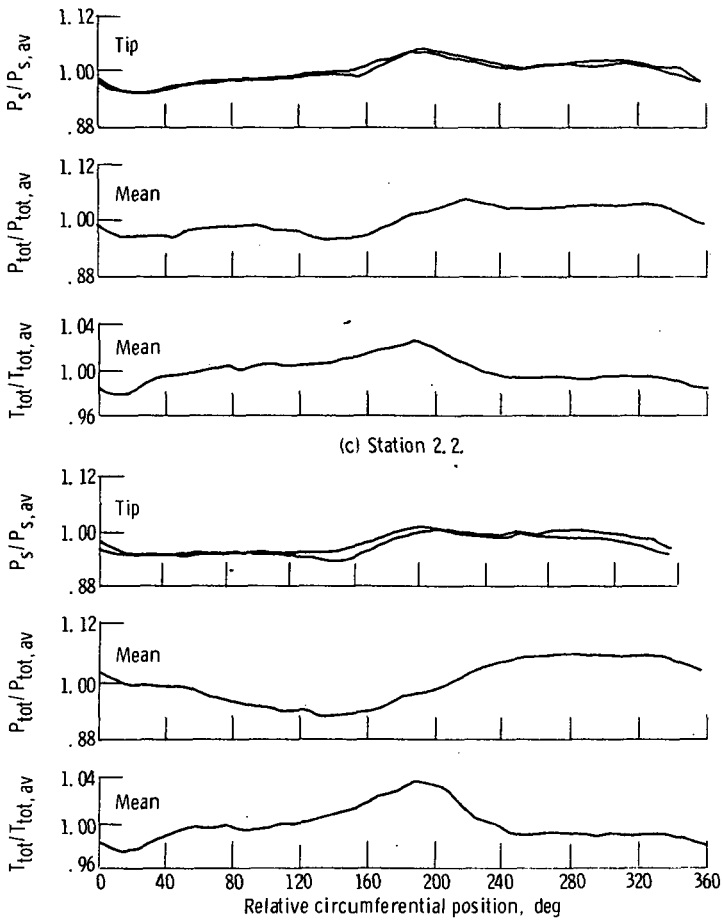

(c) Station 2.2.

(d) Station 2.3.

Figure 13. - Continued.

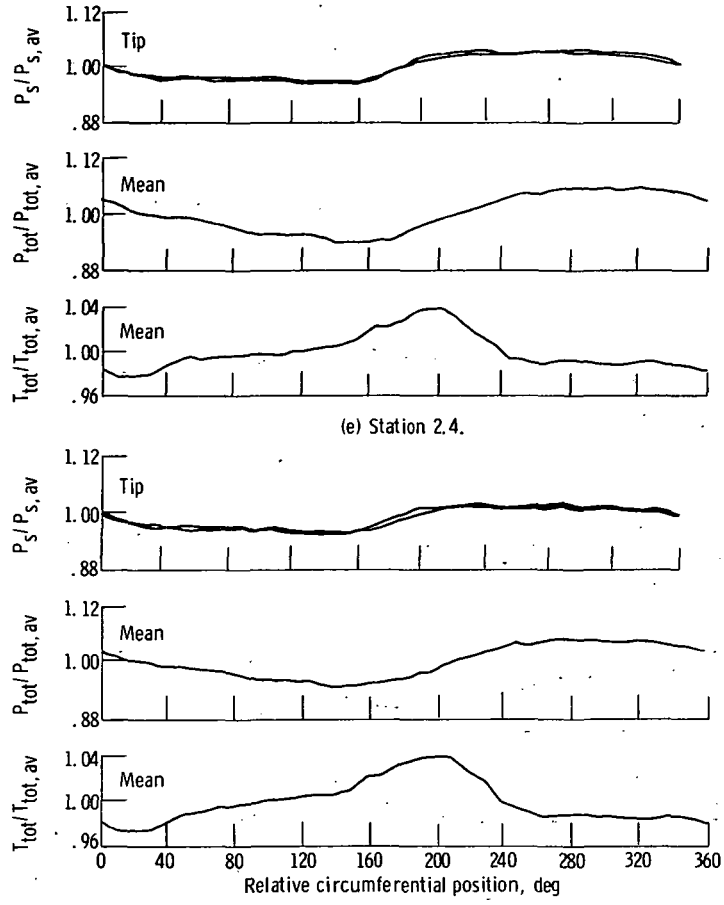

Figure 13. - Continued.

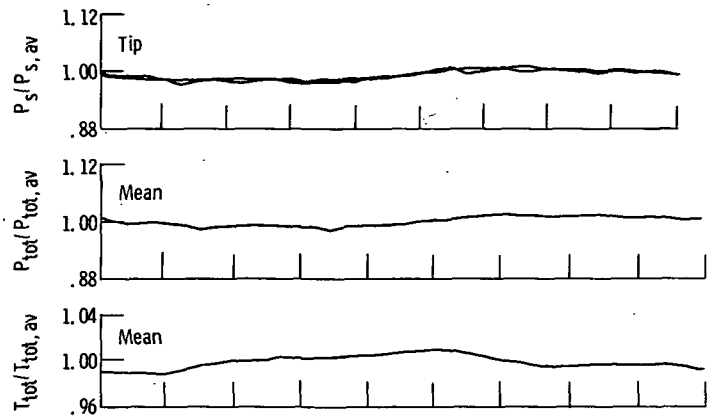

(g) Station 2.6.

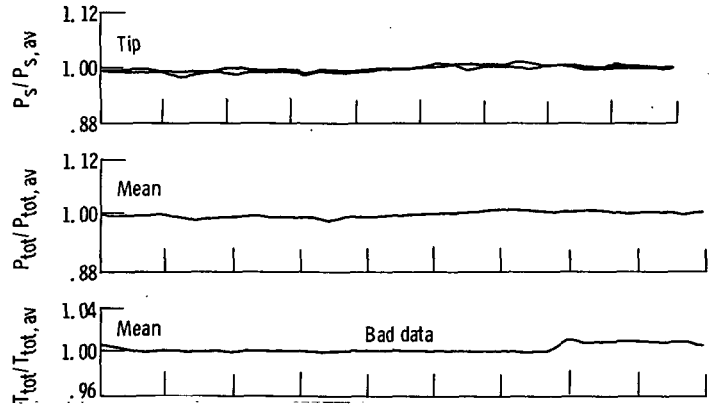

(h) Station 2.7.

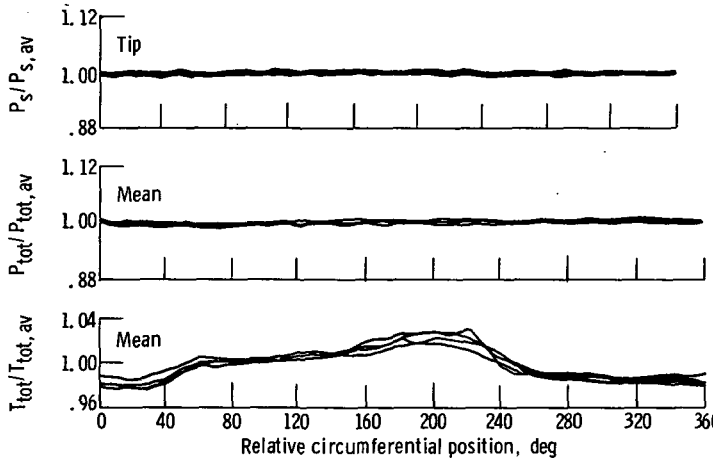

(i) Station 3.0.

Figure 13. - Concluded.

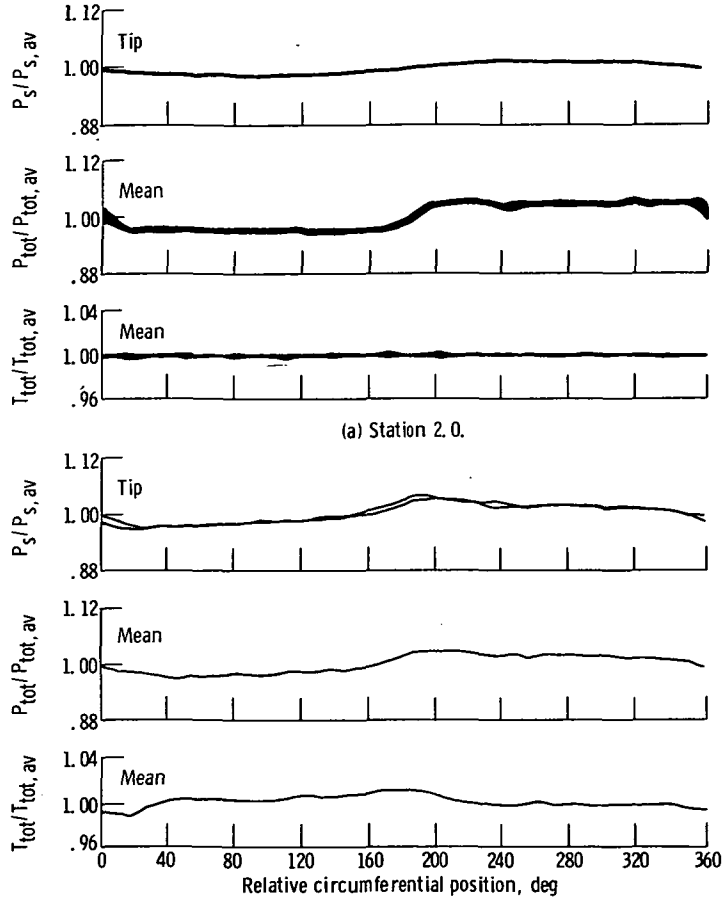

Figure 14. - Static- and total-pressure and total-temperature profiles for distorted J85-13 inlet. Rotor speed, 80 percent of design.

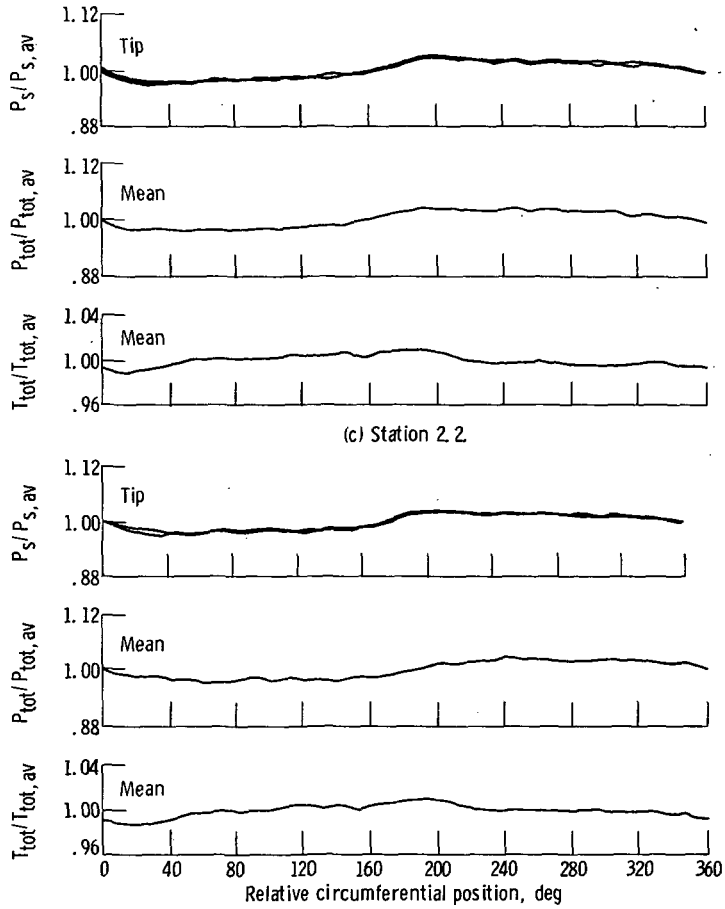

(c) Station 2.2.

(d) Station 2.3.

Figure 14. - Continued.

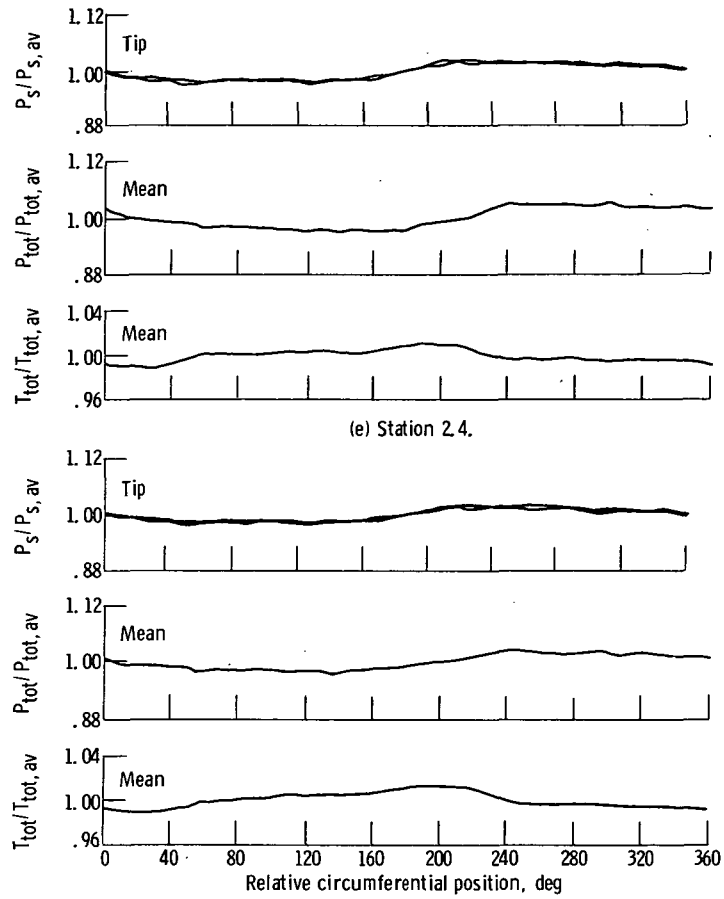

Figure 14. - Continued.

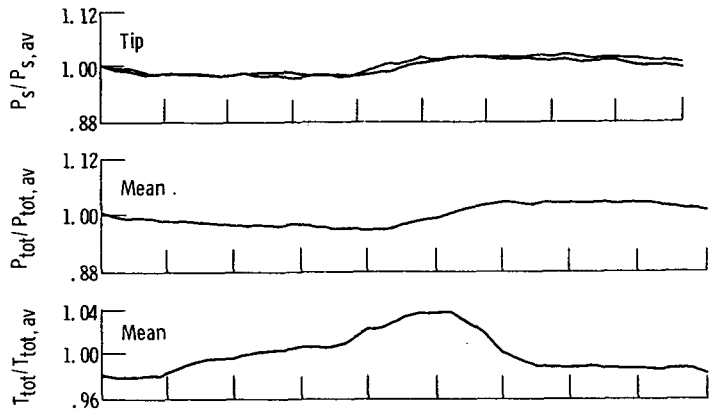

(g) Station 2.6.

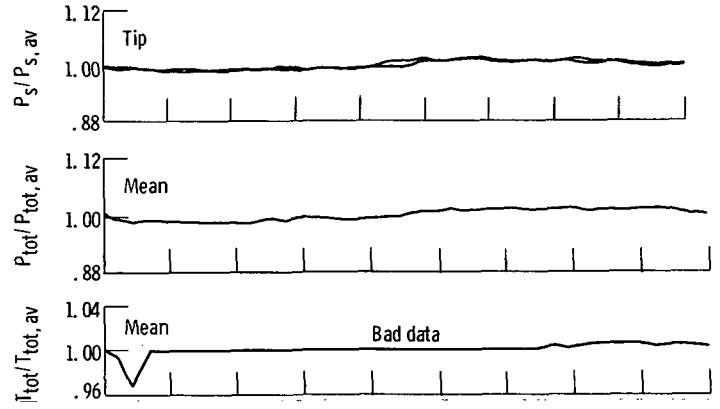

(h) Station 2.7.

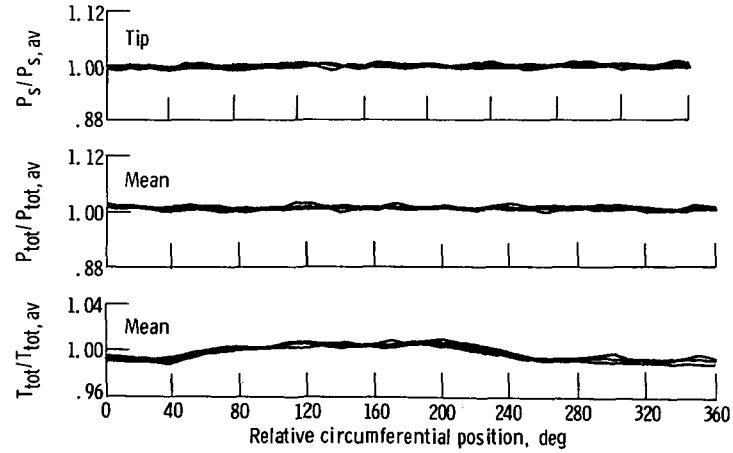

(i) Station 3.0.

Figure 14. - Concluded.

"The aeronautical and space activities of the United States shall be conducted so as to contribute . . . to the expansion of human knowledge of phenomena in the atmosphere and space. The Administration shall provide for the widest practicable and appropriate dissemination of information concerning its activities and the results thereof."

—NATIONAL AERONAUTICS AND SPACE ACT OF 1958

NASA SCIENTIFIC AND TECHNICAL PUBLICATIONS

TECHNICAL REPORTS: Scientific and technical information considered important, complete, and a lasting contribution to existing knowledge.

TECHNICAL NOTES: Information less broad in scope but nevertheless of importance as a contribution to existing knowledge.

TECHNICAL MEMORANDUMS: Information receiving limited distribution because of preliminary data, security classification, or other reasons. Also includes conference proceedings with either limited or unlimited distribution.

CONTRACTOR REPORTS: Scientific and technical information generated under a NASA contract or grant and considered an important contribution to existing knowledge.

TECHNICAL TRANSLATIONS: Information published in a foreign language considered to merit NASA distribution in English.

SPECIAL PUBLICATIONS: Information derived from or of value to NASA activities. Publications include final reports of major projects, monographs, data compilations, handbooks, sourcebooks, and special bibliographies.

TECHNOLOGY UTILIZATION PUBLICATIONS: Information on technology used by NASA that may be of particular interest in commercial and other non-aerospace applications. Publications include Tech Briefs, Technology Utilization Reports and Technology Surveys.

Details on the availability of these publications may be obtained from:

SCIENTIFIC AND TECHNICAL INFORMATION OFFICE

NATIONAL AERONAUTICS AND SPACE ADMINISTRATION

Washington, D.C. 20546